
Weakly Supervised Detection of Hallucinations in LLM Activations

Miriam Rateike
Saarland University
IBM Research Africa
Nairobi, Kenya

Celia Cintas
IBM Research Africa
Nairobi, Kenya

John Wamburu
IBM Research Africa
Nairobi, Kenya

Tanya Akumu
IBM Research Africa
Nairobi, Kenya

Skyler Speakman
IBM Research Africa
Nairobi, Kenya

Abstract

We propose an auditing method to identify whether a large language model (LLM) encodes patterns such as hallucinations in its internal states, which may propagate to downstream tasks. We introduce a weakly supervised auditing technique using a subset scanning approach to detect anomalous patterns in LLM activations from pre-trained models. Importantly, our method does not need knowledge of the type of patterns *a-priori*. Instead, it relies on a reference dataset devoid of anomalies during testing. Further, our approach enables the identification of pivotal nodes responsible for encoding these patterns, which may offer crucial insights for fine-tuning specific sub-networks for bias mitigation. We introduce two new scanning methods to handle LLM activations for anomalous sentences that may deviate from the expected distribution in either direction. Our results confirm prior findings of BERT’s limited internal capacity for encoding hallucinations, while OPT appears capable of encoding hallucination information internally. Importantly, our scanning approach, without prior exposure to false statements, performs comparably to a fully supervised out-of-distribution classifier.

1 Introduction

The rapid proliferation of Large Language Models (LLMs) has transformed the landscape of natural language processing, empowering applications ranging from chatbots and dialogue systems [57] to content generation [45, 46]. However, as these models become an integral part of our communication, there are concerns about the potential biases (e.g., hallucinations¹, toxicity, stereotypes) embedded within their outputs [14, 33, 42, 55, 59]. These subtle and implicit biases can reinforce stereotypes, marginalize certain groups, and perpetuate inequalities [7, 21]. Auditing LLMs for bias is thus essential for upholding ethical standards, reducing harm, and an inclusive deployment.

Despite advances in bias detection and mitigation strategies for LLMs in recent years, a large corpus of prior work has focused on word-level representations [5, 9, 49]. However, in recent years, sentence-level representations from models such as GPT [45, 46] have become prevalent for text sequence encoding. Moreover, prior research has primarily operated under the assumption that the particular type of bias, such as hallucinations, is known *a priori*, i.e., during the training phase [3, 32]. However, this assumption can potentially restrict these methods’ practical applicability and generalizability

¹The term “hallucinations” refers to factual errors [3].

since they rely on access to labeled data, which may necessitate a resource-intensive data collection process. Gaining access to labeled data can be particularly challenging when the occurrence of a bias is infrequent and given that language constantly evolves, which inherently leads to the continuous change of biases and their linguistic expressions. Moreover, exposure to harmful content can lead to emotional and psychological stress for content moderators/labelers [38].

In this work, we propose an auditing approach to bias detection in LLMs sentence embeddings when the bias is *not known a-priori*. Our goal is to determine if a pre-trained LLM has internalized harmful anomalous patterns (e.g., hallucinations) by examining its internal states (node activations). Following prior work [3, 24], our underlying assumption is that an LLM capable of predicting or generating anomalous content will exhibit detectable indicators of this tendency within its internal states.

Our method extends prior work on anomalous subset scanning for neural networks [12, 26, 27] by scanning pre-trained LLM activations. Our method operates without the need for training data containing labeled anomalous content (e.g., false/hallucinated statements). Unlike classifiers, we do not require a training phase for a particular bias type. Instead, during testing, we rely on a reference dataset assumed to contain “normal” (or safe) content devoid of anomalies. When testing, we input a test dataset, possibly containing bias, to a pre-trained LLM model under audit. Our method examines the LLM’s hidden states (activations) and identifies a subset of input data (e.g., sentences and nodes) as anomalous. We extend the prior work [12, 26, 27] to address that LLM embeddings for anomalous sentences may deviate in either direction from the expected distribution. If anomalous sentences, e.g., those containing stereotypes, are detected from the activations, it suggests the model encodes those anomalous patterns. Conversely, the absence of anomalies detected in the activations of anomalous sentences may indicate the model’s potential robustness to those patterns.²

1.1 Related Work

Auditing LLM Outputs. Prior work on detecting anomalies such as stereotypes, toxicity, or hallucinations in LLM models has concentrated on analyzing the model’s generated content such as the percentage of anomalous options preferred or chosen [29, 41]. Other work has explored the propagation of bias to downstream tasks, including coreference resolution [58], sentiment analysis [42], topic modeling [20], and prediction models [18]. However, the effectiveness of these approaches is heavily reliant on the quality of pre-trained downstream models. A different line of work has examined bias in the activations of LLMs, using principal component analysis [4, 32, 58], clustering [4], or training detection classifiers on the latent space [3, 4, 8, 22]. Other work has studied distance metrics between word pair representations [4, 8]. However, this approach has shown inconsistency detection results within contextual scenarios [22, 29, 35]. Furthermore, these approaches assume the availability of fully labeled training data and require predefined anomalous patterns. Few prior work has addressed the identification of unknown biases in LLMs, particularly in the context of unbiased sentence classification [52]. In this work, our goal is to detect whether an LLM encodes anomalies (e.g., hallucinations) within its hidden states. We work under the assumption that only “normal” (e.g., true) data is available, while the presence of anomalous (e.g., false) data remains undisclosed.

DeepScan In the context of analyzing data using a pre-trained network, deep subset scanning (DeepScan) [12] has been used to detect anomalous samples in various computer vision and audio tasks, including creativity sample characterization [13], audio adversarial attacks in inner layers of autoencoders [2], patch-based attacks in flow networks [27] and skin condition classification [26]. In this work, we extend prior work by scanning pre-trained LLM activations and introducing two novel methods to effectively identify anomalous sentences deviating from the expected activation distribution in either direction.

2 DeepScan for LLMs

This section introduces adaptations and extensions to deep subset scanning (DeepScan) [12, 27] for auditing LLM activations. Specifically, we detail the adaptation of previous deep scanning approaches to search for the “most anomalous” subset of node activations and input sentences within the inner layers of a pre-trained LLM network. We assume two datasets: a reference dataset \mathcal{B} containing B “normal” (e.g., factually true) sentences, and an independent test dataset \mathcal{T} containing M sentences,

²Note that we cannot confirm a null hypothesis (absence of anomalies).

which may be either “normal” or “anomalous” (e.g., factually false). A sentence can represent any continuous text span and is not limited to a traditional linguistic sentence [25].

Problem Formulation. Consider an LLM, such as BERT [25], which can generate activations through its encoder³. Assume we have M test sentences represented by a vector of activations $Z^l = [Z_1^l, \dots, Z_M^l]$ generated by the LLM at layer l , with each sentence activation having dimension J corresponding to the set of nodes $O^l = \{O_1^l, \dots, O_J^l\}$. Now, let $Z_S \subseteq Z$ and $O_S \subseteq O$, then we define a subset over sentences and nodes as $S = Z_S \times O_S$. Our goal is to identify the subset of activations containing the most anomalous (e.g., hallucinated) content based on a scoring function $F(S)$ that yields the anomaly score of a subset S : $S^* = \arg \max_S F(S)$.

Detecting anomalies in activations typically requires parametric assumptions for the scoring function (e.g., Gaussian, Poisson). However, given that the distribution of activations in specific layers can be highly skewed, we adopt a non-parametric approach, following prior work [11, 12, 26, 36, 37]. This approach, known as non-parametric scan statistics (NPSS), makes minimal assumptions about the underlying distribution of node activations. For this, we first derive p -values from the activations and then perform a scan over these p -values to quantify the difference or shift in the activation distribution for each dimension (node) compared to the reference distribution. We detail this now.

Empirical p -values. In line with prior work [12], we utilize the activations from the (“normal”) reference data \mathcal{B} to compute empirical p -values for the activations from the (“normal” or “anomalous”) test data \mathcal{T} . For a given test activation z_{mj}^{Tl} (corresponding to sentence m , layer l and node j), we calculate its empirical p -value by first sorting the set of activations from the reference data $\{z_{bj}^{Bl}\}_{b=1}^B$ corresponding to layer l and node j across all reference sentences $b = 1 \dots B$ and then determining the rank of the test activation within that sorted list of reference activations. Subsequently, we normalize these positions to generate p -values within $[0, 1]$:

$$p_{mj}^l = \frac{1 + \sum_{b=1}^B \mathbf{1}(z_{bj}^{Bl} \geq z_{mj}^{Tl})}{1 + B}. \quad (1)$$

Here, $\mathbf{1}(\cdot)$ is the indicator function. For ties, we consider both the rank on the left (pmin) and right sides (pmax). This gives us a range $[\text{pmin}, \text{pmax}]$. To obtain a single p -value within the range, we perform uniform sampling. We compute p -values for a given layer l for each node j and sentence m of the test activations.

There are different methods for computing these empirical p -values. In left-tail (right-tail) p -values, the focus is on extreme values on the left (right) side of the reference activation distribution, indicating smaller (larger) values compared to the reference dataset. For two-tailed p -values, the focus is on extreme values on both (left and right) sides. Prior research concentrated on one-tailed p -values [12, 26] on the left side of the activation distribution. However, in our case, we observe deviations on both sides of the distribution and introduce two novel methods to incorporate the extreme values from both ends, as we detail below.

Uniform Distribution of p -values Under Null Hypothesis When the null hypothesis is true, it implies that any observed data point has an equal chance of falling anywhere within the distribution of possible values under the null hypothesis [39, 48]. Therefore, when we calculate empirical p -values by determining how extreme our observed data is relative to this null distribution, each potential outcome is equally likely. This uniformity in probabilities across the distribution ensures that p -values for samples confirming the null hypothesis follow a uniform distribution, as they are essentially measuring the randomness of the data in a manner consistent with the null hypothesis’s assumptions. Thus if the test dataset were to contain only “normal” sentences (null hypothesis), the p -values for test activations at layer l would exhibit for each node j a uniform distribution across sentences. When anomalous sentences are introduced, and the LLM activations encode these anomalies, we hypothesize a departure from this uniform p -value distribution, particularly for certain nodes j .

Scoring Function. To test whether the p -value distributions diverge from a uniform distribution, we employ a scoring function based on a test statistic, denoted as $F(S) = \max_{\alpha} F_{\alpha}(S)$, where α represents a significance level, and $F_{\alpha}(S)$ is defined by a suitable goodness-of-fit statistic.

³Or decoder for decoder-only models like GPT [45, 46] or OPT [56].

In the following explanation, we closely follow [12]. The general form of the scoring function is:

$$F(S) = \max_{\alpha} F_{\alpha}(S) = \max_{\alpha} \phi(\alpha, N_{\alpha}(S), N(S)) \quad (2)$$

where $N(S)$ represents the number of empirical p -values contained in subset S , $N_{\alpha}(S)$ is the number of p -values less than (significance level) α contained in subset S , $\alpha \in (0, 1)$ is a significance level and ϕ is a goodness-of-fit statistics. To identify a subset S that presents the strongest indication of significantly exceeding the expected activation distribution under the null hypothesis (“normal” or clean data). This is expressed by the condition $N_{\alpha}(S) > \alpha N(S)$, where α denotes the chosen significance level. In our experiments, we run a grid search over $\alpha \in [0.05, 0.5]$ in steps of 0.05.

Higher Criticism Test Statistic While there are several established goodness-of-fit statistics available for use in NPSS [37], in this work, we utilize the Higher Criticism (HC) test statistic [17]:

$$\phi(\alpha, N_{\alpha}(S), N(S)) = \frac{|N_{\alpha}(S) - N(S)\alpha|}{\sqrt{N(S)\alpha(1 - \alpha)}} \quad (3)$$

This could be understood as the test statistic for a Wald test assessing the number of significant p -values, where N_{α} follows a binomial distribution with parameters N_{α} and α . Due to its normalization by the standard deviation of N_{α} , HC tends to yield smaller subsets characterized by wider ranges of p -values. This occurs because such subsets yield larger values in the numerator while generating smaller values in the denominator. In our case, small subsets are particularly preferable in scenarios where the quantity of anomalous data within the test dataset is small, as shown in our experiments (Section 3), where the test dataset comprises only 10-20% anomalous data.

Efficient Search Algorithm. To overcome the computational challenge posed by maximizing a scoring function across all possible data sample and node subsets, we employ Fast Generalized Subset Scanning (FGSS) as previously utilized in similar research [12, 26]. This approach significantly reduces the number of subsets under consideration from $O(2^E)$ to $O(E)$ within each optimization step, where E represents the number of elements currently being optimized, such as images or nodes (see Appendix C, Algorithm 2). This efficiency is based on the application of the LTSS property [43], which involves sorting each element based on its priority, defined as the proportion of p -values below a threshold α . FGSS assures convergence to a local optimum. The algorithm returns anomalous subset S^* defined by a set of nodes O_{S^*} and a subset of sentences Z_{S^*} from the test dataset, collectively defining the most anomalous pattern as a group.

Using results from both tails. We observe that LLM embeddings for anomalous data may shift from the expected reference distribution in both directions. To identify subsets marked as anomalous due to shifts to the left or right for different nodes, we introduce two novel methods to aggregate scanning results. The first approach involves aggregating results obtained from scanning left-tail and right-tail p -values. We identify subset of sentences $Z_{S_R^*}$ by scanning over right-tailed p -values and $Z_{S_L^*}$ by scanning over left-tailed p -values. We then combine these results through union: $Z_{S^*}^{\text{Union}} := Z_{S_R^*} \cup Z_{S_L^*}$. The second approach is an iterative method that combines results from scanning two-sided p -values. It aggregates the top- k subsets returned by the scanning, where after each iteration $i = 1 \dots k$, the found subset of sentences $Z_{S_i^*}$ is removed from the test dataset, and the subsequent scanning is performed on the reduced test set. The final subset is the union over all identified subsets: $Z_{S^*}^{\text{top-}k} := Z_{S_1^*} \cup Z_{S_2^*} \cup \dots \cup Z_{S_k^*}$.

3 Experimental Setup and Results

This section presents experimental results for bias detection in LLMs using our two proposed scanning methods. We focus on hallucination detection and analyze the subset of input sentences returned. For additional results on toxicity and stereotype detection, refer to Appendix E.

Data and LLM Models. We use an English-language dataset Hallucinations [3] (‘Cities’ topic) containing factually true (e.g., “Nakuru is a city in Kenya.”) and false statements (e.g., “Surrey is a city in Kenya.”). We use a test dataset of 800 samples comprising 10% anomalous data, reflecting the real-world scarcity of such data. We sample test data 10 times with replacement from a larger pool of data and report mean and standard deviation. For further details regarding the dataset selection

LLM	Layer	Clf	Precision	Recall	Size
BERT	10	clf+	0.099 (0.006)	0.73 (0.046)	0.737 (0.01)
		scan2	0.114 (0.022)	0.631 (0.105)	0.563 (0.075)
		scanLR	0.091 (0.017)	0.61 (0.062)	0.685 (0.075)
	12	clf+	0.128 (0.017)	0.428 (0.059)	0.335 (0.012)
		scan2	0.085 (0.011)	0.392 (0.062)	0.459 (0.018)
		scanLR	0.065 (0.029)	0.465 (0.246)	0.695 (0.074)
OPT	20	clf+	0.33 (0.018)	0.742 (0.041)	0.225 (0.01)
		scan2	0.16 (0.057)	0.734 (0.2)	0.479 (0.065)
		scanLR	0.45 (0.034)	0.605 (0.055)	0.134 (0.01)
	24	clf+	0.274 (0.015)	0.752 (0.034)	0.275 (0.013)
		scan2	0.149 (0.031)	0.685 (0.096)	0.471 (0.094)
		scanLR	0.693 (0.272)	0.418 (0.146)	0.076 (0.042)

Table 1: Comparison of our weakly supervised scan methods unions: left- and right-tailed p -value scans (scanLR), and top-3 two-tailed p -value scans (scan2), and the supervised out-of-distribution classifier baseline (clf+) on auditing BERT and OPT. Performance and relative subset (Size) reported as mean (std) across 10 random test datasets with 10% anomalous data. Best (significant) bold.

and preprocessing, see Appendix A. We audit two pre-trained LLMs: the BERT base (uncased) model [16] with a 12-layer encoder with 768 nodes per layer, where focus on activations for the [CLS] token, and the Facebook OPT 6.7 model [56] with a 32-layer decoder with 4096 nodes per layer. Note that our method can audit any LLM that provides activations. For details, see Appendix B.

DeepScan Extensions and Baseline. We scan over left-, right-, and two-tailed p -values. Building upon prior work [3], we analyze the activations from layers closer to the output as they are suspected of encoding higher-level information. For further details, see Appendix C. We report results for the introduced scanning extensions: the outcomes derived from the combined subset of left and right p -value scans (scanLR), along with the results from the top-3 scan over the two-sided p -values (scan2). To evaluate our detection power, we compare to a supervised classifier (clf+) that aims to predict whether a sentence is true or false based on the LLM activation [3]. It is trained for each LLM layer on an approximately balanced dataset containing 1739 false sentences and is tested on an out-of-distribution held-out dataset (e.g., other topics) of the same task. For details, see Appendix D.

Results. We present results in Table 1. After identifying the subset, we assume access to test labels and report precision, and recall. Precision measures the ability to avoid false positives, calculated as the ratio of correctly identified anomalous samples to the total samples flagged as anomalous. Recall quantifies the ability to find all anomalous sentences, measured as the ratio of correctly identified anomalous samples to the total actual anomalous instances. We also report the size of the subgroup of sentences returned by the scanner or the number of sentences predicted as false by the classifier.

We first audit BERT. Across activations from both layer 10 and (last) layer 12, we observe low precision across all methods. These results indicate that BERT has a limited capacity to represent hallucinations within its internal state effectively, confirming prior work [3]. Subsequently, we audit OPT, a more potent model designed to match GPT’s capabilities [56]. We consistently observe higher precision in detecting false statements across methods and test sets. From an auditing perspective, these findings indicate that OPT does indeed encode hallucination information within its internal state. This is consistent with prior research [3], which found layer 20 to be the most predictive for their classifier. Yet, our scanning approach (scanLR) excels at layer 24.

Comparing methods, scan2 achieves similar precision levels to the classifier for BERT. At layer 10, the classifier shows highest recall while flagging $\sim 74\%$ of sentences as false, despite an expected rate of 10%, indicating a high False Positive Rate. In the case of OPT, scanLR exhibits higher precision than the supervised baseline for layer 20, with a subset size ($\sim 13\%$) closely matching the expected 10%. Nevertheless, scan2 and clf+ achieve the highest recall rates and return larger subsets for both layers. In summary, method effectiveness varies with test dataset and layers, without a clear dominant method. Rather, we observe a trade-off between precision and recall, with one method excelling in precision at the cost of recall, and vice versa. We also observe a strong connection between subset

size and recall, where larger subsets tend to yield higher recall but often at the cost of decreased precision. In conclusion, our method—with no prior exposure to false statements—exhibits similar performance to an out-of-distribution classifier trained on larger amounts of anomalous samples when both are assessed using a dataset comprising just 10% anomalous data (80 samples).

4 Summary and Discussion

We have introduced a weakly supervised auditing technique to identify, whether a pre-trained LLM is encoding patterns such as hallucinations within its internal states. We are interested in this problem because if an LLM is encoding these patterns internally, it can potentially impact downstream tasks and one may be able to deploy bias mitigation strategies. Our method employs subset scanning across various neural network layers in pre-trained LLMs, without the need for prior knowledge of the specific patterns or access to labeled false statements.

During validation on a hallucination dataset, our approach achieved performance similar to, and sometimes surpassing a baseline fully supervised out-of-distribution classifier. Importantly, our approach only requires access to samples labeled as “normal” (true) eliminating the need for anomalous pattern data, which can be costly and ethically challenging to obtain (especially for other types of anomalies, such as toxicity and stereotypes). This makes our method highly suitable for real-world applications. Nonetheless, recent research [31] has raised doubts about the generalizability of prior methods [3, 10] in detecting hallucinations, which we intend to explore further. Our work makes assumptions about the background dataset, assuming it *only* contains “normal” statements tailored to the problem at hand. We plan to extend our work to more realistic assumptions by including small amounts of anomalous data in the reference dataset and composing it of various data sources.

Finally, similar to work using metrics such as cosine-similarity [32], our method only has positive predictive ability: it can be used to detect the presence of anomalies but not their absence. To understand how much of our experimental results can be attributed to our method’s detection power and how much is due to the LLM not encoding the anomalous pattern, we have compared it to a supervised baseline. Our results indeed show that our method, which requires no training and no prior exposure to false statements, performs comparably to the supervised baseline.

5 Outlook: Informing Fine-tuning

We briefly discuss the potential expansion of our work. Unsupervised pre-training and task-specific fine-tuning have become the standard approach for various LLM tasks [19, 23, 50]. Despite their impressive achievements, these methods face challenges in generalization performance on downstream tasks [25, 30, 44] and suffer from catastrophic forgetting [1, 34, 54]. To address these issues, sub-network optimization approaches have emerged as a promising method to enhance stability and reduce overfitting without requiring full network retraining [51, 54].

We believe that our method can build on the advancement of this line of research for bias mitigation strategies. As detailed in § 2, our method allows identifying the subset of nodes O_{S^*} that are most responsible for the anomalous patterns found. This means, for each layer, we are able to identify the nodes that align with the most anomalous subset of sentences, that is those nodes for which the empirical p -values of their activations deviate from the uniform distribution such that they are flagged anomalous. This suggests that these nodes are pivotal in identifying anomalous patterns within the data, which could guide the efficient fine-tuning of sub-networks for bias mitigation strategies. We show initial findings in Appendix E.

Acknowledgements

We appreciate Amos Azaria and Tom Mitchell for sharing their data and code. Special thanks to Edward McFowland III for valuable feedback and discussions.

References

- [1] Armen Aghajanyan, Akshat Shrivastava, Anchit Gupta, Naman Goyal, Luke Zettlemoyer, and Sonal Gupta. Better fine-tuning by reducing representational collapse. In *International Conference on Learning Representations*, 2021.
- [2] Victor Akinwande, Celia Cintas, Skyler Speakman, and Srihari Sridharan. Identifying audio adversarial examples via anomalous pattern detection. *arXiv preprint arXiv:2002.05463*, 2020.
- [3] Amos Azaria and Tom Mitchell. The internal state of an llm knows when its lying. *arXiv preprint arXiv:2304.13734*, 2023.
- [4] Christine Basta, Marta R Costa-jussà, and Noe Casas. Evaluating the underlying gender bias in contextualized word embeddings. In *Proceedings of the First Workshop on Gender Bias in Natural Language Processing*, pages 33–39, 2019.
- [5] Christine Basta, Marta R Costa-Jussa, and Noe Casas. Extensive study on the underlying gender bias in contextualized word embeddings. *Neural Computing and Applications*, 33(8):3371–3384, 2021.
- [6] Robert H Berk and Douglas H Jones. Goodness-of-fit test statistics that dominate the kolmogorov statistics. *Zeitschrift für Wahrscheinlichkeitstheorie und verwandte Gebiete*, 47(1):47–59, 1979.
- [7] Abeba Birhane, Vinay Prabhhu, Sang Han, and Vishnu Naresh Boddeti. On hate scaling laws for data-swamps. *arXiv preprint arXiv:2306.13141*, 2023.
- [8] Tolga Bolukbasi, Kai-Wei Chang, James Y Zou, Venkatesh Saligrama, and Adam T Kalai. Man is to computer programmer as woman is to homemaker? debiasing word embeddings. *Advances in neural information processing systems*, 29, 2016.
- [9] Shikha Bordia and Samuel Bowman. Identifying and reducing gender bias in word-level language models. In *Proceedings of the 2019 Conference of the North American Chapter of the Association for Computational Linguistics: Student Research Workshop*, pages 7–15, 2019.
- [10] Collin Burns, Haotian Ye, Dan Klein, and Jacob Steinhardt. Discovering latent knowledge in language models without supervision. *arXiv preprint arXiv:2212.03827*, 2022.
- [11] Feng Chen and Daniel B Neill. Non-parametric scan statistics for event detection and forecasting in heterogeneous social media graphs. In *Proceedings of the 20th ACM SIGKDD international conference on Knowledge discovery and data mining*, pages 1166–1175, 2014.
- [12] Celia Cintas, Skyler Speakman, Victor Akinwande, William Ogallo, Komminist Weldemariam, Srihari Sridharan, and Edward McFowland. Detecting adversarial attacks via subset scanning of autoencoder activations and reconstruction error. In *Proceedings of the Twenty-Ninth International Conference on International Joint Conferences on Artificial Intelligence*, pages 876–882, 2021.
- [13] Celia Cintas, Payel Das, Brian Quanz, Girmaw Abebe Tadesse, Skyler Speakman, and Pin-Yu Chen. Towards creativity characterization of generative models via group-based subset scanning. In *International Joint Conference on Artificial Intelligence*, 2022.
- [14] Ameet Deshpande, Vishvak Murahari, Tanmay Rajpurohit, Ashwin Kalyan, and Karthik Narasimhan. Toxicity in chatgpt: Analyzing persona-assigned language models. *arXiv preprint arXiv:2304.05335*, 2023.
- [15] Sunipa Dev, Akshita Jha, Jaya Goyal, Dinesh Tewari, Shachi Dave, and Vinodkumar Prabhakaran. Building stereotype repositories with llms and community engagement for scale and depth. *Cross-Cultural Considerations in NLP@ EACL*, page 84, 2023.
- [16] Jacob Devlin, Ming-Wei Chang, Kenton Lee, and Kristina Toutanova. BERT: pre-training of deep bidirectional transformers for language understanding. *CoRR*, abs/1810.04805, 2018. URL <http://arxiv.org/abs/1810.04805>.
- [17] David Donoho and Jiashun Jin. Higher criticism for detecting sparse heterogeneous mixtures. *The Annals of Statistics*, 32(3):962–994, 2004.
- [18] Samuel Gehman, Suchin Gururangan, Maarten Sap, Yejin Choi, and Noah A Smith. Realtoxicityprompts: Evaluating neural toxic degeneration in language models. In *Findings of the Association for Computational Linguistics: EMNLP 2020*, pages 3356–3369, 2020.

- [19] Muhammad Usman Hadi, R Qureshi, A Shah, M Irfan, A Zafar, MB Shaikh, N Akhtar, J Wu, and S Mirjalili. A survey on large language models: Applications, challenges, limitations, and practical usage. *TechRxiv*, 2023.
- [20] Saad Hassan, Matt Huenerfauth, and Cecilia Ovesdotter Alm. Unpacking the interdependent systems of discrimination: Ableist bias in nlp systems through an intersectional lens. *Findings of the Association for Computational Linguistics: EMNLP 2021*, 2021.
- [21] Peter Henderson, Koustuv Sinha, Nicolas Angelard-Gontier, Nan Rosemary Ke, Genevieve Fried, Ryan Lowe, and Joelle Pineau. Ethical challenges in data-driven dialogue systems. In *Proceedings of the 2018 AAAI/ACM Conference on AI, Ethics, and Society*, pages 123–129, 2018.
- [22] Alexander Henlein and Alexander Mehler. What do toothbrushes do in the kitchen? how transformers think our world is structured. In *Proceedings of the 2022 Conference of the North American Chapter of the Association for Computational Linguistics: Human Language Technologies*, pages 5791–5807, 2022.
- [23] Hanyao Huang, Ou Zheng, Dongdong Wang, Jiayi Yin, Zijin Wang, Shengxuan Ding, Heng Yin, Chuan Xu, Renjie Yang, Qian Zheng, et al. Chatgpt for shaping the future of dentistry: the potential of multi-modal large language model. *International Journal of Oral Science*, 15(1):29, 2023.
- [24] Mohsen Jamali, Ziv M Williams, and Jing Cai. Unveiling theory of mind in large language models: A parallel to single neurons in the human brain. *arXiv preprint arXiv:2309.01660*, 2023.
- [25] Jacob Devlin Ming-Wei Chang Kenton and Lee Kristina Toutanova. Bert: Pre-training of deep bidirectional transformers for language understanding. In *Proceedings of NAACL-HLT*, pages 4171–4186, 2019.
- [26] Hannah Kim, Girmaw Abebe Tadesse, Celia Cintas, Skyler Speakman, and Kush Varshney. Out-of-distribution detection in dermatology using input perturbation and subset scanning. In *2022 IEEE 19th International Symposium on Biomedical Imaging (ISBI)*, pages 1–4. IEEE, 2022.
- [27] Hannah Kim, Celia Cintas, Girmaw Abebe Tadesse, and Skyler Speakman. Spatially constrained adversarial attack detection and localization in the representation space of optical flow networks. In Edith Elkind, editor, *Proceedings of the Thirty-Second International Joint Conference on Artificial Intelligence, IJCAI-23*, pages 965–973. International Joint Conferences on Artificial Intelligence Organization, 8 2023. doi: 10.24963/ijcai.2023/107. URL <https://doi.org/10.24963/ijcai.2023/107>. Main Track.
- [28] Taeuk Kim, Kang Min Yoo, and Sang-goo Lee. Self-guided contrastive learning for bert sentence representations. In *Proceedings of the 59th Annual Meeting of the Association for Computational Linguistics and the 11th International Joint Conference on Natural Language Processing (Volume 1: Long Papers)*, pages 2528–2540, 2021.
- [29] Keita Kurita, Nidhi Vyas, Ayush Pareek, Alan W Black, and Yulia Tsvetkov. Measuring bias in contextualized word representations. In *Proceedings of the First Workshop on Gender Bias in Natural Language Processing*, pages 166–172, 2019.
- [30] Cheolhyoung Lee, Kyunghyun Cho, and Wanmo Kang. Mixout: Effective regularization to finetune large-scale pretrained language models. In *International Conference on Learning Representations (ICLR)*. International Conference on Learning Representations, 2020.
- [31] BA Levinstein and Daniel A Herrmann. Still no lie detector for language models: Probing empirical and conceptual roadblocks. *arXiv preprint arXiv:2307.00175*, 2023.
- [32] Paul Pu Liang, Irene Mengze Li, Emily Zheng, Yao Chong Lim, Ruslan Salakhutdinov, and Louis-Philippe Morency. Towards debiasing sentence representations. In *Proceedings of the 58th Annual Meeting of the Association for Computational Linguistics*, pages 5502–5515, 2020.
- [33] Yang Liu, Yuanshun Yao, Jean-Francois Ton, Xiaoying Zhang, Ruocheng Guo Hao Cheng, Yegor Klochkov, Muhammad Faaiz Taufiq, and Hang Li. Trustworthy llms: a survey and guideline for evaluating large language models’ alignment. *arXiv preprint arXiv:2308.05374*, 2023.
- [34] Rabeeh Karimi Mahabadi, Yonatan Belinkov, and James Henderson. Variational information bottleneck for effective low-resource fine-tuning. *arXiv preprint arXiv:2106.05469*, 2021.

- [35] Chandler May, Alex Wang, Shikha Bordia, Samuel Bowman, and Rachel Rudinger. On measuring social biases in sentence encoders. In *Proceedings of the 2019 Conference of the North American Chapter of the Association for Computational Linguistics: Human Language Technologies, Volume 1 (Long and Short Papers)*, pages 622–628, 2019.
- [36] Edward McFowland, Skyler Speakman, and Daniel B Neill. Fast generalized subset scan for anomalous pattern detection. *The Journal of Machine Learning Research*, 14(1):1533–1561, 2013.
- [37] Edward McFowland III, Sriram Somanchi, and Daniel B Neill. Efficient discovery of heterogeneous treatment effects in randomized experiments via anomalous pattern detection. *arXiv preprint arXiv:1803.09159*, 2018.
- [38] Milagros Miceli and Julian Posada. The data-production dispositif. *Proceedings of the ACM on Human-Computer Interaction*, 6(CSCW2):1–37, 2022.
- [39] Duncan J Murdoch, Yu-Ling Tsai, and James Adcock. P-values are random variables. *The American Statistician*, 62(3):242–245, 2008.
- [40] Moin Nadeem, Anna Bethke, and Siva Reddy. Stereoset: Measuring stereotypical bias in pretrained language models. In *Proceedings of the 59th Annual Meeting of the Association for Computational Linguistics and the 11th International Joint Conference on Natural Language Processing (Volume 1: Long Papers)*, pages 5356–5371, 2021.
- [41] Nikita Nangia, Clara Vania, Rasika Bhalerao, and Samuel R Bowman. Crows-pairs: A challenge dataset for measuring social biases in masked language models. In *2020 Conference on Empirical Methods in Natural Language Processing, EMNLP 2020*, pages 1953–1967. Association for Computational Linguistics (ACL), 2020.
- [42] Pranav Narayanan Venkit, Sanjana Gautam, Ruchi Panchanadikar, Ting-Hao Huang, and Shomir Wilson. Unmasking nationality bias: A study of human perception of nationalities in ai-generated articles. In *Proceedings of the 2023 AAAI/ACM Conference on AI, Ethics, and Society*, pages 554–565, 2023.
- [43] Daniel B. Neill. Fast subset scan for spatial pattern detection. *Journal of the Royal Statistical Society (Series B: Statistical Methodology)*, 74(2):337–360, 2012.
- [44] Jason Phang, Thibault Févry, and Samuel R Bowman. Sentence encoders on stilts: Supplementary training on intermediate labeled-data tasks. *arXiv preprint arXiv:1811.01088*, 2018.
- [45] Alec Radford, Karthik Narasimhan, Tim Salimans, Ilya Sutskever, et al. Improving language understanding by generative pre-training. 2018.
- [46] Alec Radford, Jeffrey Wu, Rewon Child, David Luan, Dario Amodei, Ilya Sutskever, et al. Language models are unsupervised multitask learners. *OpenAI blog*, 1(8):9, 2019.
- [47] Nils Reimers and Iryna Gurevych. Sentence-bert: Sentence embeddings using siamese bert-networks. In *Proceedings of the 2019 Conference on Empirical Methods in Natural Language Processing and the 9th International Joint Conference on Natural Language Processing (EMNLP-IJCNLP)*. Association for Computational Linguistics, 2019.
- [48] John A Rice. *Mathematical statistics and data analysis*. Thomson Brooks/Cole, 2007.
- [49] Yi Chern Tan and L Elisa Celis. Assessing social and intersectional biases in contextualized word representations. *Advances in neural information processing systems*, 32, 2019.
- [50] Arun James Thirunavukarasu, Darren Shu Jeng Ting, Kabilan Elangovan, Laura Gutierrez, Ting Fang Tan, and Daniel Shu Wei Ting. Large language models in medicine. *Nature medicine*, pages 1–11, 2023.
- [51] Shoujie Tong, Heming Xia, Damai Dai, Tianyu Liu, Binghuai Lin, Yunbo Cao, and Zhifang Sui. Bi-drop: Generalizable fine-tuning for pre-trained language models via adaptive subnetwork optimization. *arXiv preprint arXiv:2305.14760*, 2023.
- [52] PA Utama, NS Moosavi, and I Gurevych. Towards debiasing nlu models from unknown biases. In *Proceedings of the 2020 Conference on Empirical Methods in Natural Language Processing (EMNLP 2020)*, pages 7597–7610. Association for Computational Linguistics, 2020.
- [53] Andrew Wang, Mohit Sudhakar, and Yangfeng Ji. Simple text detoxification by identifying a linear toxic subspace in language model embeddings. *arXiv preprint arXiv:2112.08346*, 2021.

- [54] Runxin Xu, Fuli Luo, Zhiyuan Zhang, Chuanqi Tan, Baobao Chang, Songfang Huang, and Fei Huang. Raise a child in large language model: Towards effective and generalizable fine-tuning. In *Proceedings of the 2021 Conference on Empirical Methods in Natural Language Processing*, pages 9514–9528, 2021.
- [55] Jingfeng Yang, Hongye Jin, Ruixiang Tang, Xiaotian Han, Qizhang Feng, Haoming Jiang, Bing Yin, and Xia Hu. Harnessing the power of llms in practice: A survey on chatgpt and beyond. *arXiv preprint arXiv:2304.13712*, 2023.
- [56] Susan Zhang, Stephen Roller, Naman Goyal, Mikel Artetxe, Moya Chen, Shuohui Chen, Christopher Dewan, Mona Diab, Xian Li, Xi Victoria Lin, Todor Mihaylov, Myle Ott, Sam Shleifer, Kurt Shuster, Daniel Simig, Punit Singh Koura, Anjali Sridhar, Tianlu Wang, and Luke Zettlemoyer. Opt: Open pre-trained transformer language models, 2022.
- [57] Yizhe Zhang, Siqi Sun, Michel Galley, Yen-Chun Chen, Chris Brockett, Xiang Gao, Jianfeng Gao, Jingjing Liu, and William B Dolan. Dialogpt: Large-scale generative pre-training for conversational response generation. In *Proceedings of the 58th Annual Meeting of the Association for Computational Linguistics: System Demonstrations*, pages 270–278, 2020.
- [58] Jieyu Zhao, Tianlu Wang, Mark Yatskar, Ryan Cotterell, Vicente Ordonez, and Kai-Wei Chang. Gender bias in contextualized word embeddings. In *Proceedings of the 2019 Conference of the North American Chapter of the Association for Computational Linguistics: Human Language Technologies*, volume 1, 2019.
- [59] Terry Yue Zhuo, Yujin Huang, Chunyang Chen, and Zhenchang Xing. Red teaming chatgpt via jailbreaking: Bias, robustness, reliability and toxicity. *arXiv preprint arXiv:2301.12867*, pages 12–2, 2023.

A Datasets

This section provides additional information on the datasets used and their curation for our use.

A.1 Hallucinations Dataset

The Hallucinations dataset [3]⁴ provides a collection of true and false statements across six domains: Cities, Inventions, Chemical Elements, Animals, Companies, and Scientific Facts. The dataset has been curated by the authors using reliable sources utilized to craft true statements while corresponding false statements are generated using distinct values from the same source. The dataset maintains the same amount of true and false statements for each topic. The authors express their intention to release the dataset publicly and have kindly granted us access in advance. The dataset consists of a total of six topics: Cities (7573 samples after deleting duplicates), Inventions (876), (Chemical) Elements (930), Animals (1008), Companies (1200), and (Scientific) Facts (612). We use the Cities dataset as test data. Importantly, when we mention “hallucinations” data hereinafter, we assume it pertains to the Cities topic unless specified otherwise. We evenly divide the true statements into the reference and clean batches while utilizing the false statements as the anomalous batch.

A.2 RealToxicityPrompts Dataset

The RealToxicityPrompts dataset [18] comprises 100,000 sentence snippets sourced from the web. Each instance includes a prompt and a continuation. The prompt includes attributes such as text, profanity, sexually explicit content, identity attack, flirtation, threat, insult, severe toxicity, and toxicity scores. The dataset is structured to offer insights into various aspects of toxicity. The scores accompanying the prompt and continuation are calculated using the Perspective API. The prompts were selected from sentences in the OPEN-WEBTEXT CORPUS, with toxicity scores $([0, 1])$ extracted using the PERSPECTIVE API⁵. The dataset was curated to ensure a stratified representation of prompt toxicity across different ranges.

We rely on a test dataset provided by HuggingFace⁶, comprising 99442 samples. We concatenate the prompt and the continuation, subsequently deriving the toxicity score by calculating the average of the scores from both sentences. If a score is not available for a continuation, we rely on the toxicity score from the prompt. We first split the dataset into harmless and toxic sentences. As prior work [53], we assume sentences with a toxicity score below 0.3 as harmless scores and sentences with a toxicity score above 0.7. We split the dataset into three non-overlapping batches: reference (22479 samples), clean (22479 samples), and anomalous (3642 samples). For the experiments, we reduced the reference and clean sample size to 2000 sentences.

A.3 Stereoset Dataset

The Stereoset [40] dataset is designed to assess stereotype bias in language models and comprises 17000 sentences that evaluate model preferences across gender, race, religion, and profession. It supports tasks like multiple-choice question answering. The dataset is available in English and is structured into intersentence and intrasentence categories. Each data instance contains information such as the bias type (e.g., gender, race), context sentence, and target sentence. The dataset also includes gold labels indicating whether sentences are `stereotypical`, `anti-stereotypical`, or `unrelated`. The data was collected through crowdworkers, with annotations provided by 475 and 803 annotators for intrasentence and intersentence tasks, respectively. The dataset’s focus on measuring bias within various domains underscores its relevance for evaluating language model fairness and comprehension. Note that the stereotypes are grounded in US contexts, and some sentences generated by annotators may be objectively false or include favorable stereotypes. Recent work emphasizes the importance of community engagement to enhance dataset curation strategies, addressing challenges in achieving comprehensive representation across diverse global cultures and perspectives when building stereotype repositories [15].

⁴The authors generously provided us with access to the dataset upon our request.

⁵<https://github.com/conversationai/perspectiveapi>

⁶<https://huggingface.co/datasets/allenai/real-toxicity-prompts>

We rely on a validation dataset provided by HuggingFace⁷, comprising 2123 samples for intersentence, and 2106 samples for intrasentence. Our approach involves random sampling from our dataset to form reference, clean, and anomalous batches. Each batch comprises 702 samples, while we ensure that sentences do not overlap within each batch. In this context, we define `unrelated` as representing the normal data, while `stereotypical` signifies the anomalous pattern. For the `intrasentence` scenario, we select the appropriate sentence from the dataset (`unrelated` or `stereotypical`). For the `intersentence` scenario, we generate sentence samples by combining the context sentence with the corresponding sentence continuation (`unrelated` or `stereotypical`).

B LLM Models

This section provides additional details on the large language models (LLMs) audited in our experiments.

BERT base We use the BERT base model (uncased) [16] provided by HuggingFace⁸, which is a pre-trained transformer model designed for the English language, and the corresponding Tokenizer. BERT is trained via self-supervised training on unlabeled raw texts, utilizing two objectives: masked language modeling and next-sentence prediction. Its training data includes a large corpus of English texts, and it is important to note that the model can have biased predictions. The model has been primarily designed for fine-tuning downstream tasks such as sequence classification and token classification.

BERT is constructed as a transformer-based model, which employs an encoder architecture with a self-attention mechanism that allows it to capture contextual information from both preceding and following words in a sentence, creating a bidirectional understanding. The BERT base model encoder has 12 layers, and 12 attention heads per layer. The embedded space of the model has a dimension of 768. In BERT, the `[CLS]` token is a special token added to the beginning of each input sequence. The final hidden state of the `[CLS]` token is often used as a summary representation of the entire input sequence for downstream classification tasks. Our analysis focuses on the hidden representations of the `[CLS]` token, as it is commonly used for downstream classification tasks [28, 47].

OPT We use the Open Pre-trained Transformer (OPT) language model [56] (6.7B) provided by HuggingFace⁹. It has been specifically trained to align with the performance and sizes of the GPT-3 models employing causal language modeling (CLM) objectives. The training data for OPT comprises a fusion of filtered datasets sourced from various origins, such as BookCorpus, CC-Stories, The Pile, Reddit, and CCNewsV2, which is comprised mainly of English text, with a small quantity of non-English data. OPT serves multiple purposes, including text generation and evaluation via prompts, and can be fine-tuned for specific tasks. The training of the pre-trained model spanned approximately 33 days and harnessed the power of multiple GPUs. Note that the model is susceptible to biases and safety concerns due to its training on a diverse and unfiltered array of internet data.

The model utilizes a decoder-only pre-trained transformer architecture. It consists of 32 layers, where each layer is composed of 4096 hidden units. For a data and model card, see [56].

C Scanner Details and Setup

This section provides additional details on the setup of our scanning approach. For more details see prior work [12, 26].

Visual Exploration of Activations and Empirical p -values In § 2, we stated that to detect anomalies in activations we would typically need to rely on parametric assumptions, but due to the potential skewness in specific layer activations, we prefer to rely on a non-parametric approach with minimal assumptions about the underlying distribution of activations. Instead, we detect anomalies in p -values derived from activations. We expect the p -values from clean samples to be uniformly distributed, while we expect the p -values from anomalous samples not to be distributed uniformly.

⁷<https://huggingface.co/datasets/stereoset>

⁸<https://huggingface.co/bert-base-uncased>

⁹<https://huggingface.co/facebook/opt-6.7b>

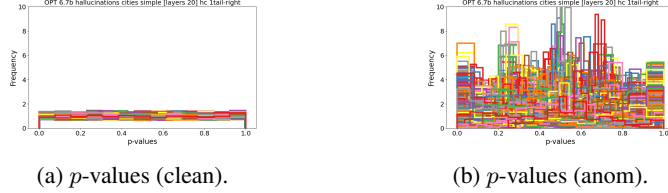


Figure 1: Distributions right-tailed empirical p -values for activations from all 4096 nodes (colors) of OPT 6.7b layer 20 over test samples from Hallucinations data. Clean samples refer to true statements, and anomalous (anom) samples refer to false statements.

We provide a visual exploration of this concept in Figure 1. Specifically, we study the p -values derived from activations from OPT 6.7b activations in layer 20, using the hallucination dataset. Each node’s distribution is depicted in a distinct color. We examine the distribution of empirical p -values computed under the reference dataset (containing “clean”) statements for clean (Fig. 1a) and anomalous (Fig. 1b) data. We observe that the p -values under the null hypothesis (“clean” data) exhibit a uniform distribution, whereas the p -values for the anomalous data significantly deviate from uniformity. Our method leverages this difference in p -value distributions to identify anomalous patterns.

Berk Jones Test Statistic In Appendix E, we also report results that use the Berk-Jones (BJ) test statistic [6]:

$$\phi(\alpha, N_\alpha(S), N(S)) = N(S)KL\left(\frac{N_\alpha(S)}{N(S)}, \alpha\right), \quad (4)$$

where KL is the Kullback-Leibler divergence $KL(x, y) = x \log \frac{x}{y} + (1 - x) \log \frac{1-x}{1-y}$ between the observed and expected proportions of significant p -values.

Fast Generalized Subset Scanning Algorithm We follow prior work [12, 26] in employing an iterative optimization process to identify anomalous subsets of p -values (see Algorithm 1 and Algorithm 2).

Algorithm 1 Single Restart over M test sentences and J nodes

```

1: procedure SINGLERESTART( $(M \times J)$   $p$ -values)
2:   score  $\leftarrow -1$ 
3:    $Z_s \leftarrow \text{RANDOM}(M)$ 
4:    $O_s \leftarrow \text{RANDOM}(J)$ 
5:   while score is increasing do
6:      $(M' \times J') = (M \times J)|_{O_s}$ 
7:     score,  $Z_s \leftarrow \text{OPTIMIZEROWS}((M \times J'))$ 
8:      $(M' \times J) = (M \times J)|_{Z_s}$ 
9:     score,  $O_s \leftarrow \text{OPTIMIZEROWS}((J \times M'))$ 
10:  end while
11:  return score,  $Z_s, O_s$ 
12: end procedure

```

D Additional Information on Experiments

In this section, we provide additional information on the experiments, especially reporting test, reference, and training dataset sizes. Finally, we also report details on the code and computational resources used to run experiments.

D.1 Test Data for Scanner and Classifier

For testing purposes, we select for Hallucinations and RealToxicityPrompts datasets a total of 800 samples from both clean and anomalous data at varying proportions as specified in our experiments.

Algorithm 2 Optimize over rows using LTSS (*OptimizeRows*). It maintains maxscore and maxsubset over $\|E\| * \|T\|$ subsets.

```
1: procedure OPTIMIZEROWS( $p$ -values from all rows  $E$  and relevant cols  $C$ )
2:   maxscore  $\leftarrow -1$ 
3:   maxsubset  $\leftarrow \emptyset$ 
4:   for  $t$  in  $T = \text{LINEARSPACE}(0,1)$  do
5:     sortedpriority  $\leftarrow \text{SORTBYPROPCT}(E, t)$ 
6:     Score(sortedpriority,  $t$ )
7:   end for
8:   return maxscore, maxsubset
9: end procedure
```

To illustrate, in the case of a 90 : 10 split, we draw 90% of the 800 samples from the clean dataset, and 10% of the 800 samples from the anomalous dataset, also containing 2000 samples. For the Stereoset dataset, we chose a total of 400 samples from clean and anomalous data (each containing a total of 500 samples) across various mixing variations as described above.

D.2 Reference Dataset for Scanner

The reference, clean, and anomalous datasets contain 2000 samples for RealToxicityPrompts, 1500 samples for Hallucinations, and 500 for Stereoset.

D.3 Training Data for Classifier

Following [3], the baseline classifier is trained to predict whether a sentence is anomalous or not based on the LLM hidden layer’s values. The classifier is composed of four fully connected layers featuring ReLU activation functions and a progressively decreasing number of neurons (256, 128, 64). The final layer employs a sigmoid activation function for binary classification. Training is conducted over 5 epochs with a batch size of 32, using the Adam optimizer and a 80 : 20 training-validation split.

We train two types of classifiers classifier, one trained on the datasets from the same distribution as the test dataset (clf^*) and one trained on a different distribution than the test dataset (clf^+). We train clf^* on Hallucinations (topic: Cities) using 989 anomalous, and 989 clean samples. For training clf^+ on Hallucinations (topics: Inventions, Elements, Animals, Facts) we use 1739 anomalous, and 1688 clean samples.

In Appendix E, we provide additional results for RealToxicityPrompts and Stereoset data. Due to the lack of a suitable out-of-distribution dataset, we report the results of in-distribution classifiers as a fully supervised best-method comparison. Specifically, we train clf^* on Stereoset (inter-sentence, normal: unrelated, anomalous: stereotypes) using 208 anomalous, and 415 clean samples. We train clf^* on RealToxicityPrompts (normal: toxicity score in $[0, 0.3]$, anomalous: toxicity score $[0.7, 1]$) using 1642 anomalous, and 2000 clean samples.

D.4 Computational Resources and Code

All experiments were conducted on a MacBook Pro (Apple M1 Max chip). For our code, we rely on the publicly available GitHub repository: <https://github.com/Trusted-AI/adversarial-robustness-toolbox/tree/main/art/defences/detector/evasion/subsetsscanning>.

E Additional Results

In this section, we present the following additional results:

- In E.1, we provide additional results for the RealToxicityPrompts dataset.
- In E.2, we provide additional results for the Stereoset dataset.
- In E.3, we provide additional results for test datasets with larger amounts of anom. data.

- In E.4, we offer additional insights into our proposed `scanLR` method.
- In E.5, we offer additional insights into our proposed `scan2` method.
- In E.6, we explore the returned subset of nodes, as introduced in § 5.

Metrics. After identifying the subset, we assume access to test labels and calculate the following performance metrics

- Precision measures the ability to avoid false positives, calculated as the ratio of correctly identified anomalous samples to the total samples flagged as anomalous.
- Recall quantifies the ability to find all anomalous sentences, measured as the ratio of correctly identified anomalous samples to the total actual anomalous instances.
- For classifiers, we also sometimes report accuracy reported by prior work [3]. Accuracy measures the overall correctness of the classification, calculated as the ratio of correctly classified samples—both anomalous and “normal”—to the total number of test samples.

Note that accuracy takes both true positives and true negatives into account, but it may not be as informative in highly imbalanced datasets where the number of “normal” instances significantly outweighs the anomalous ones (as in the case reported in the main paper). In such cases, precision and recall are often more informative metrics.

Additionally, we include the measurement of the proportion of samples identified as anomalous or biased in relation to the size of the test set. As the subset size increases (i.e., an increase in both True Positives and False Positives), recall tends to increase as it becomes more likely that the model will correctly identify more of the positive samples.

Methods We compare the following methods:

- `scanL` : Conducts a group scan over one-tailed left-sided empirical p -values obtained from activations.
- `scanR` : Conducts a group scan over one-tailed right-sided empirical p -values obtained from activations as prior work [12, 26].
- `scanLR`: Our first proposed method performs a group scan that combines `scanL` and `scanR` and returns the union of the anomalous subset of sentences detected by each individual method (see § 2).
- `scan2`: Our second proposed novel method conducts a top- k group scan over two-tailed empirical p -values obtained from activations and unions the found subsets (see § 2).
- `c1f+` is the out-of-distribution classifier proposed by prior work [3]

E.1 Additional Results on RealToxicityPrompts

In Table 2 we report additional information on the performance of our two proposed scanning methods (`scanLR`, `scan2`) on the RealToxicityPrompts dataset described in Section A. Note that due to the lack of out-of-distribution data, we do not report a baseline classifier (`c1f+`).

We observe that, similar to the other datasets, precision is at its lowest when dealing with 10% of anomalous data, but it improves as the amount of anomalous data increases. Additionally, we notice that recall shows an upward trend as the subset size of flagged anomalous data grows, as expected. In general, we observe that `scan2` $k=3$ exhibits the highest recall, which is expected, as we aggregate results over the top-3 outcomes enlarging the subset size.

E.2 Additional Results on Stereoset

In Table 3 we report additional information on the performance of our two proposed scanning methods (`scanLR`, `scan2`) on the Stereoset dataset described in Section A. Note that due to the lack of out-of-distribution data, we do not report a baseline classifier (`c1f+`).

We observe that, similar to the other datasets, precision is at its lowest when dealing with 10% of anomalous data, but it improves as the amount of anomalous data increases. For BERT, precision

LLM	Anom	Layer	Method	Precision	Recall	Size	
BERT	10%	10	scan2 k1	0.121 (0.028)	0.205 (0.058)	0.169 (0.018)	
			scan2 k2	0.129 (0.02)	0.442 (0.071)	0.343 (0.014)	
			scan2 k3	0.127 (0.012)	0.581 (0.046)	0.458 (0.028)	
			scanLR	0.12 (0.026)	0.228 (0.067)	0.188 (0.025)	
		12	scan2 k1	0.12 (0.104)	0.094 (0.059)	0.106 (0.066)	
			scan2 k2	0.084 (0.021)	0.244 (0.08)	0.292 (0.078)	
			scan2 k3	0.091 (0.016)	0.37 (0.061)	0.411 (0.044)	
			scanLR	0.145 (0.128)	0.095 (0.049)	0.112 (0.067)	
		20%	10	scan2 k1	0.238 (0.022)	0.206 (0.028)	0.173 (0.019)
				scan2 k2	0.256 (0.023)	0.451 (0.056)	0.352 (0.017)
				scan2 k3	0.259 (0.021)	0.612 (0.062)	0.473 (0.029)
				scanLR	0.27 (0.03)	0.446 (0.199)	0.322 (0.128)
	50%	12	scan2 k1	0.199 (0.117)	0.084 (0.057)	0.092 (0.065)	
			scan2 k2	0.168 (0.042)	0.234 (0.082)	0.28 (0.079)	
			scan2 k3	0.192 (0.031)	0.388 (0.088)	0.402 (0.045)	
			scanLR	0.244 (0.144)	0.199 (0.286)	0.156 (0.185)	
	10%	10	scan2 k1	0.57 (0.027)	0.204 (0.019)	0.179 (0.016)	
			scan2 k2	0.61 (0.028)	0.452 (0.03)	0.372 (0.03)	
			scan2 k3	0.611 (0.013)	0.599 (0.04)	0.49 (0.034)	
			scanLR	0.641 (0.033)	0.418 (0.171)	0.324 (0.126)	
		20%	12	scan2 k1	0.491 (0.046)	0.089 (0.049)	0.092 (0.051)
				scan2 k2	0.48 (0.043)	0.26 (0.053)	0.271 (0.054)
				scan2 k3	0.568 (0.052)	0.454 (0.077)	0.398 (0.04)
				scanLR	0.66 (0.058)	0.446 (0.327)	0.319 (0.229)
20%		10%	scan2 k1	0.144 (0.01)	0.365 (0.032)	0.254 (0.015)	
			scan2 k2	0.128 (0.011)	0.534 (0.048)	0.418 (0.012)	
			scan2 k3	0.127 (0.013)	0.58 (0.06)	0.458 (0.017)	
			scanLR	0.145 (0.01)	0.427 (0.046)	0.294 (0.023)	
	28%	scan2 k1	0.146 (0.014)	0.386 (0.065)	0.263 (0.026)		
		scan2 k2	0.135 (0.008)	0.577 (0.061)	0.427 (0.028)		
		scan2 k3	0.133 (0.009)	0.64 (0.054)	0.48 (0.028)		
		scanLR	0.193 (0.01)	0.48 (0.129)	0.252 (0.074)		
	50%	24%	scan2 k1	0.265 (0.022)	0.35 (0.032)	0.264 (0.015)	
			scan2 k2	0.247 (0.015)	0.522 (0.029)	0.424 (0.016)	
			scan2 k3	0.252 (0.02)	0.598 (0.06)	0.473 (0.023)	
			scanLR	0.315 (0.049)	0.455 (0.106)	0.303 (0.092)	
28%		scan2 k1	0.288 (0.014)	0.394 (0.039)	0.274 (0.026)		
		scan2 k2	0.277 (0.021)	0.591 (0.057)	0.429 (0.049)		
		scan2 k3	0.266 (0.02)	0.654 (0.055)	0.492 (0.033)		
		scanLR	0.384 (0.024)	0.311 (0.164)	0.159 (0.073)		
50%		24%	scan2 k1	0.594 (0.022)	0.347 (0.035)	0.292 (0.031)	
			scan2 k2	0.639 (0.02)	0.472 (0.034)	0.37 (0.03)	
			scan2 k3	0.599 (0.012)	0.634 (0.024)	0.53 (0.021)	
			scanLR	0.745 (0.045)	0.208 (0.022)	0.14 (0.015)	
	28%	scan2 k1	0.629 (0.023)	0.379 (0.041)	0.302 (0.033)		
		scan2 k2	0.651 (0.026)	0.501 (0.044)	0.386 (0.044)		
		scan2 k3	0.607 (0.013)	0.658 (0.022)	0.542 (0.022)		
		scanLR	0.717 (0.036)	0.239 (0.019)	0.166 (0.008)		

Table 2: Results for the RealToxicityPrompts dataset. Comparison of our weakly supervised scan methods union of left- and right-tailed p -values (scanLR) and top- k for $k \in \{1, 2, 3\}$ two-tailed p -value scans (scan2) on auditing BERT and OPT. Mean (std) results from 10 random test datasets, with best (significant) results in bold. Results for test sets with different percentages of anomalous data (Anom), different layers (Layers), and size of data flagged/classified anomalous relative to the test dataset (Size).

LLM	Anom	Layer	Method	Precision	Recall	Size
BERT	10%	10	scan2 k2	0.119 (0.016)	0.405 (0.084)	0.168 (0.023)
			scan2 k3	0.123 (0.013)	0.515 (0.066)	0.21 (0.016)
			scan2 k4	0.125 (0.015)	0.558 (0.065)	0.223 (0.017)
			scanLR	0.136 (0.017)	0.26 (0.034)	0.192 (0.007)
		12	scan2 k2	0.156 (0.01)	0.52 (0.073)	0.167 (0.024)
			scan2 k3	0.13 (0.009)	0.572 (0.076)	0.221 (0.024)
			scan2 k4	0.129 (0.009)	0.61 (0.059)	0.237 (0.016)
			scanLR	0.142 (0.04)	0.245 (0.111)	0.164 (0.045)
	20%	10	scan2 k2	0.255 (0.024)	0.439 (0.098)	0.17 (0.028)
			scan2 k3	0.271 (0.018)	0.581 (0.062)	0.215 (0.022)
			scan2 k4	0.261 (0.017)	0.621 (0.049)	0.239 (0.017)
			scanLR	0.279 (0.038)	0.285 (0.038)	0.204 (0.009)
		12	scan2 k2	0.286 (0.018)	0.521 (0.055)	0.182 (0.017)
			scan2 k3	0.262 (0.023)	0.594 (0.051)	0.228 (0.026)
			scan2 k4	0.253 (0.013)	0.644 (0.038)	0.255 (0.02)
			scanLR	0.274 (0.032)	0.255 (0.085)	0.183 (0.045)
	50%	10	scan2 k2	0.626 (0.031)	0.509 (0.041)	0.203 (0.012)
			scan2 k3	0.654 (0.018)	0.676 (0.043)	0.258 (0.016)
			scan2 k4	0.638 (0.018)	0.721 (0.045)	0.283 (0.02)
			scanLR	0.666 (0.043)	0.321 (0.04)	0.242 (0.036)
		12	scan2 k2	0.627 (0.015)	0.564 (0.047)	0.225 (0.02)
			scan2 k3	0.605 (0.013)	0.629 (0.046)	0.26 (0.021)
			scan2 k4	0.599 (0.013)	0.649 (0.046)	0.271 (0.02)
			scanLR	0.725 (0.041)	0.577 (0.071)	0.4 (0.06)
OPT	10 %	24	scan2 k2	0.099 (0.009)	0.432 (0.111)	0.218 (0.046)
			scan2 k3	0.101 (0.009)	0.495 (0.1)	0.246 (0.041)
			scan2 k4	0.103 (0.011)	0.532 (0.096)	0.259 (0.037)
			scanLR	0.097 (0.011)	0.375 (0.072)	0.389 (0.072)
		28	scan2 k2	0.124 (0.018)	0.455 (0.082)	0.182 (0.013)
			scan2 k3	0.118 (0.014)	0.515 (0.059)	0.218 (0.009)
			scan2 k4	0.117 (0.012)	0.55 (0.063)	0.235 (0.008)
			scanLR	0.131 (0.029)	0.395 (0.099)	0.298 (0.018)
	20%	24	scan2 k2	0.209 (0.017)	0.474 (0.131)	0.226 (0.058)
			scan2 k3	0.208 (0.018)	0.526 (0.119)	0.252 (0.05)
			scan2 k4	0.207 (0.019)	0.55 (0.12)	0.265 (0.046)
			scanLR	0.266 (0.049)	0.607 (0.203)	0.446 (0.081)
		28	scan2 k2	0.237 (0.023)	0.471 (0.094)	0.197 (0.026)
			scan2 k3	0.234 (0.021)	0.539 (0.084)	0.229 (0.02)
			scan2 k4	0.231 (0.02)	0.568 (0.075)	0.245 (0.017)
			scanLR	0.282 (0.05)	0.495 (0.173)	0.342 (0.062)
50%	24	scan2 k2	0.546 (0.016)	0.639 (0.141)	0.291 (0.059)	
		scan2 k3	0.544 (0.019)	0.662 (0.126)	0.303 (0.052)	
		scan2 k4	0.539 (0.015)	0.673 (0.117)	0.311 (0.049)	
		scanLR	0.878 (0.013)	0.93 (0.024)	0.53 (0.018)	
	28	scan2 k2	0.556 (0.02)	0.536 (0.104)	0.241 (0.042)	
		scan2 k3	0.554 (0.016)	0.583 (0.087)	0.262 (0.037)	
		scan2 k4	0.554 (0.017)	0.606 (0.08)	0.273 (0.035)	
		scanLR	0.886 (0.009)	0.912 (0.009)	0.514 (0.01)	

Table 3: Results for the Stereoset dataset. Comparison of our weakly supervised scan methods union of left- and right-tailed p -values (scanLR) top- k (for $k \in \{2, 3, 4\}$) two-tailed p -value scans (scan2). Mean (std) results from 10 random test datasets, with best (significant) results in bold. Results for test sets with different percentages of anomalous data (Anom), different layers (Layers), and size of data flagged/classified anomalous relative to the test dataset (Size).

Data	Anom	Method	F	Precision	Recall	Size
RealToxicityPrompts	50%	scan2 k3	bj	0.597 (0.015)	0.648 (0.024)	0.543 (0.021)
			hc	0.599 (0.012)	0.634 (0.024)	0.53 (0.021)
		scan2 k4	bj	0.584 (0.015)	0.694 (0.029)	0.594 (0.025)
			hc	0.587 (0.013)	0.672 (0.023)	0.572 (0.018)
		scanLR	hc	0.74 (0.04)	0.196 (0.023)	0.133 (0.015)
			bj	0.743 (0.036)	0.183 (0.022)	0.123 (0.014)
	80%	scan2 k3	bj	0.857 (0.009)	0.652 (0.017)	0.609 (0.018)
			hc	0.86 (0.01)	0.639 (0.021)	0.595 (0.022)
		scan2 k4	bj	0.849 (0.007)	0.738 (0.055)	0.697 (0.055)
			hc	0.854 (0.012)	0.678 (0.018)	0.637 (0.022)
		scanLR	hc	0.918 (0.026)	0.188 (0.021)	0.164 (0.018)
			bj	0.919 (0.029)	0.178 (0.018)	0.156 (0.014)
90%	scan2 k3	bj	0.928 (0.007)	0.638 (0.026)	0.62 (0.026)	
		hc	0.929 (0.004)	0.64 (0.044)	0.621 (0.043)	
	scan2 k4	bj	0.927 (0.005)	0.739 (0.064)	0.718 (0.062)	
		hc	0.927 (0.006)	0.677 (0.022)	0.658 (0.022)	
	scanLR	hc	0.966 (0.014)	0.184 (0.02)	0.172 (0.018)	
		bj	0.965 (0.015)	0.177 (0.014)	0.166 (0.013)	
Stereoset	50%	scan2 k3	bj	0.54 (0.012)	0.814 (0.11)	0.377 (0.053)
			hc	0.544 (0.019)	0.662 (0.126)	0.303 (0.052)
		scan2 k4	bj	0.539 (0.012)	0.817 (0.108)	0.38 (0.053)
			hc	0.539 (0.015)	0.673 (0.117)	0.311 (0.049)
		scanLR	hc	0.877 (0.015)	0.943 (0.023)	0.537 (0.016)
			bj	0.884 (0.009)	0.951 (0.012)	0.538 (0.007)
	80%	scan2 k3	bj	0.839 (0.011)	0.745 (0.122)	0.356 (0.06)
			hc	0.847 (0.01)	0.755 (0.078)	0.357 (0.035)
		scan2 k4	bj	0.836 (0.011)	0.783 (0.115)	0.376 (0.056)
			hc	0.846 (0.011)	0.764 (0.073)	0.362 (0.032)
		scanLR	hc	0.97 (0.005)	0.936 (0.01)	0.774 (0.009)
			bj	0.975 (0.006)	0.94 (0.013)	0.774 (0.012)
90%	scan2 k3	bj	0.923 (0.007)	0.792 (0.103)	0.387 (0.05)	
		hc	0.931 (0.01)	0.742 (0.093)	0.359 (0.043)	
	scan2 k4	bj	0.923 (0.007)	0.797 (0.098)	0.39 (0.048)	
		hc	0.928 (0.012)	0.75 (0.089)	0.364 (0.04)	
	scanLR	hc	0.987 (0.004)	0.935 (0.01)	0.855 (0.011)	
		bj	0.988 (0.005)	0.942 (0.008)	0.861 (0.009)	

Table 4: Results for larger percentages of anomalous data (Anom) in the test set and different test statistics: Higher Criticism (hc) and Berk Jones (bj). Results for OPT layer 24 and our weakly supervised scan methods: union of left- and right-tailed p -values (scanLR), and top- k for $k \in \{2, 3\}$ two-tailed p -value scans (scan2). Mean (std) results from 10 random test datasets, with best (significant) results in bold. Performance metrics (precision and recall), and size of data flagged anomalous relative to the test dataset (Size).

appears higher for Stereoset than RealToxicityPrompts in the previous section. Additionally, we notice that recall shows an upward trend as the subset size of flagged anomalous data grows, as expected. In general, we observe that scan2 k3 exhibits the highest recall, which is expected, as we aggregate results over the top-3 outcomes enlarging the subset size.

E.3 Additional Results on Different Testset Compositions

In Table 4 we report additional information on the performance of our two proposed scanning methods (scanLR, scan2) and the baseline classifier (clf+) for test datasets that contain larger amounts of anomalous data (50%, 80%, and 95%). We compare the results from the main paper obtained using the Higher Criticism Test, which typically favors smaller subsets, with those obtained using the Berk-Jones Test statistic, which tends to favor larger subset sizes.

In our main paper, we exclusively present findings based on test datasets that contain limited quantities of anomalous data. Our rationale for this approach stems from the presumption that anomalous data is exceedingly scarce. However, our results demonstrate across datasets that the greater the availability of anomalous data during testing, the better our method excels. For example, for RealToxicityPrompts data with 90% for `scan2` top-4 scanning with BJ scoring function, which reports 0.9727 with a recall of 0.739, while we report approximately 70% anomalous samples, while expecting 80%. For Stereoset `scanLR` BJ reports for 90% anomalous data approximately 86% with precision of 0.988 and recall of 0.942.

In this regard, our method differs from a classifier, the performance of which remains unaffected by the quantity of anomalous data within the test dataset as it operates on a per-sentence basis. Our method, instead, takes into consideration the entire dataset, identifying patterns that span across multiple sentences and nodes. Our results show that this empowers our approach to uncover patterns in BERT activations that the classifier misses. Importantly, even in scenarios characterized by a scarcity of anomalous data, should we require a test dataset containing 50% or more anomalous data, our method may still be more data efficient than a classifier. While a classifier demands not only anomalous samples in its training data but also a substantial training dataset containing a sufficient number of anomalous samples, our method does not require training data at all.

As an illustration, in line with prior work [3], we employed a dataset comprising approximately 50% anomalous samples to train their classifier `clf+`. Specifically, this training set consisted of 1739 samples for Hallucinations. We tested the classifier and our scanning method on a dataset containing only 10% anomalous data, totaling 80 samples assuming a total of 800 test samples. In this case, even if we were to consider a test dataset with 90% anomalous data, which would consist of 720 samples, it becomes apparent that our method requires fewer samples than the process of training the classifier and subsequently testing it on a dataset featuring 10% anomalous data.

In the context of auditing, where the objective is to ascertain whether a Language Model (LLM) encodes specific patterns in its internal states, we can indeed assume test datasets tailored for auditing purposes, featuring larger amounts of anomalous data. This shows that our method enables more data-efficient and precise pattern detection within LLMs than the classifier.

E.4 Additional Results for Our `scanLR` Method

In Table 5 we report additional information on the performance of our proposed scanning method `scanLR`, which unions results from scanning over left-tailed p -values (`scanL`) and results from scanning over right-tailed p -values (`scanR`). We report not only performance metrics but also the intersection of the returned nodes. We report results across all three datasets.

First, we note that the precision of individual scans (L and R) tends to be higher than when considering their union (LR), which aligns with expectations since the union incorporates false positive samples from both individual scans. However, as anticipated, the recall increases as we include more true positives from the individual scans. Specifically, we observe that LLM activations for anomalous data exhibit a tendency to shift in both directions relative to the expected “normal” distribution. Consequently, the union of scans tends to capture more anomalous data increasing recall at a slight cost to precision.

For instance, in the case of RealToxicityPrompts, when the dataset contains 10% anomalous data, we observe a slight drop in precision, going from L 0.161 and R 0.155 to LR 0.153. In contrast, we observe a substantial increase in recall, approximately 10 percentage points, from L 0.379 and R 0.39 to LR 0.48.

Regarding the intersection of the subset of nodes (INode), we notice a reduction in the node intersection as the proportion of anomalous data in the test set increases. Take, for example, the case of RealToxicityPrompts. When the dataset contains 10% anomalous data, the subset of nodes returned by individual scans (L and R) exhibits a mean intersection of 113.2 nodes, with a notable standard deviation of 108.115. However, for the dataset containing 50% anomalous data, the intersection dwindles to zero nodes, with no variance observed. This phenomenon can be attributed to the fact that, when the test set contains only a small fraction of anomalous data, the scans perform weaker in identifying patterns. Conversely, when more anomalous data is present, our scanning methods excel at detecting stronger patterns that span across sentences and nodes. The left- and right-tailed p -values concentrate on extreme deviations to the left and right of the anticipated distribution, respectively.

D	A	M	Precision	Recall	Size	INode
Hallucinations	10	L	0.205 (0.27)	0.264 (0.058)	0.218 (0.077)	-
		R	0.462 (0.37)	0.329 (0.07)	0.143 (0.104)	-
		LR	0.191 (0.095)	0.462 (0.131)	0.29 (0.122)	113.2 (108.115)
	20	L	1.0 (0.0)	0.257 (0.044)	0.052 (0.009)	-
		R	0.922 (0.233)	0.27 (0.033)	0.075 (0.064)	-
		LR	0.931 (0.206)	0.288 (0.069)	0.078 (0.074)	10.5 (31.5)
	50	L	1.0 (0.0)	0.255 (0.023)	0.128 (0.012)	-
		R	1.0 (0.0)	0.256 (0.023)	0.128 (0.011)	-
		LR	1.0 (0.0)	0.256 (0.023)	0.128 (0.011)	0.0 (0.0)
RealToxicityPrompts	10	L	0.161 (0.019)	0.379 (0.095)	0.239 (0.064)	-
		R	0.155 (0.019)	0.39 (0.045)	0.252 (0.021)	-
		LR	0.153 (0.017)	0.48 (0.087)	0.312 (0.029)	650.8 (88.062)
	20	L	0.325 (0.048)	0.33 (0.096)	0.211 (0.073)	-
		R	0.321 (0.045)	0.369 (0.103)	0.238 (0.078)	-
		LR	0.317 (0.041)	0.416 (0.13)	0.272 (0.098)	406.4 (283.095)
	50	L	0.742 (0.039)	0.188 (0.023)	0.126 (0.015)	-
		R	0.742 (0.038)	0.191 (0.02)	0.129 (0.014)	-
		LR	0.74 (0.04)	0.196 (0.023)	0.133 (0.015)	0.0 (0.0)
Stereoset	10	L	0.101 (0.017)	0.29 (0.073)	0.289 (0.064)	-
		R	0.096 (0.018)	0.268 (0.052)	0.279 (0.012)	-
		LR	0.092 (0.013)	0.345 (0.068)	0.374 (0.055)	289.3 (58.83)
	20	L	0.242 (0.065)	0.407 (0.221)	0.318 (0.088)	-
		R	0.227 (0.054)	0.299 (0.084)	0.261 (0.02)	-
		LR	0.235 (0.054)	0.464 (0.205)	0.381 (0.087)	302.6 (78.32)
	50	L	0.908 (0.011)	0.899 (0.04)	0.495 (0.02)	-
		R	0.897 (0.011)	0.914 (0.029)	0.509 (0.018)	-
		LR	0.877 (0.015)	0.943 (0.023)	0.537 (0.016)	0.6 (1.02)

Table 5: Additional results for our proposed scanLR method. Comparison of scanning over individual left-tailed p -values (L) and right-tailed p -values (R) and our proposed union of the results (LR). Mean (std) results from 10 random test datasets, with best (significant) results in bold. Results for different datasets (D), test sets with different percentages of anomalous data (A) in %, different layers (Layers). We report performance (precision, recall) and size of data flagged as anomalous relative to the test dataset (Size). For scanLR, we report the intersection of the returned subset of nodes (INode) out of 4092.

Our results suggest that certain nodes tend to shift activations to the right, while others shift to the left, and each of these shifts is detected separately by the corresponding scans.

E.5 Additional Results for Our scan2 top-k Method

In Table 6, we present additional insights into the performance of our proposed scanning method, scan2, which utilizes the top- k approach described in the main paper. In this table, we not only report performance metrics but also showcase the intersection of returned node and sentence subsets for top- k results, with k ranging from 1 to 5. We report results across all three datasets.

Importantly, in the main paper, we considered k as a hyperparameter and selected the top-3 results due to their superior performance. In certain practical scenarios, we may aim to assess methods using unlabeled data known to contain anomalous samples, yet lacking specific labels distinguishing “normal” from “anomalous” instances. In this case, determining the optimal value of k may require a different approach. To find a suitable value of k in such scenarios, one approach would involve monitoring the evolution of the anomaly score associated with the identified subset as we increment the value of k . A high score indicates a higher degree of anomaly detected within the subset. Therefore, for smaller values of k , we anticipate a higher anomaly score. As we progressively increase k and consequently remove more data identified as anomalous, the score is expected to decrease. At a certain value of k , the score may experience a drop, at which point we could select the k just before this decrease in scores as the best choice.

Data	Anom	k	Precision	Recall	Size (S)	Size (N)	INode
Hallucinations	10%	1	0.813 (0.293)	0.267 (0.036)	0.047 (0.042)	0.149 (0.134)	0 (0)
		2	0.233 (0.118)	0.502 (0.08)	0.247 (0.085)	0.496 (0.09)	0.523 (0.151)
		3	0.149 (0.031)	0.685 (0.096)	0.471 (0.094)	0.747 (0.042)	0.653 (0.065)
		4	0.142 (0.033)	0.919 (0.069)	0.675 (0.134)	0.828 (0.041)	0.602 (0.045)
		5	0.113 (0.014)	0.946 (0.034)	0.854 (0.118)	0.897 (0.033)	0.57 (0.055)
	20%	1	1.0 (0.0)	0.256 (0.043)	0.051 (0.009)	0.073 (0.005)	0 (0)
		2	0.711 (0.295)	0.543 (0.083)	0.183 (0.08)	0.301 (0.202)	0.44 (0.311)
		3	0.412 (0.094)	0.736 (0.072)	0.379 (0.099)	0.613 (0.117)	0.614 (0.131)
		4	0.337 (0.027)	0.899 (0.049)	0.537 (0.05)	0.777 (0.021)	0.672 (0.057)
		5	0.26 (0.024)	0.928 (0.046)	0.72 (0.072)	0.86 (0.019)	0.624 (0.044)
	50%	1	1.0 (0.0)	0.254 (0.022)	0.127 (0.011)	0.074 (0.003)	0 (0)
		2	1.0 (0.0)	0.512 (0.031)	0.256 (0.015)	0.102 (0.004)	0.544 (0.383)
		3	0.779 (0.041)	0.754 (0.041)	0.486 (0.039)	0.508 (0.037)	0.646 (0.139)
		4	0.683 (0.023)	0.943 (0.032)	0.692 (0.043)	0.771 (0.014)	0.73 (0.048)
		5	0.595 (0.04)	0.969 (0.03)	0.818 (0.065)	0.853 (0.011)	0.656 (0.037)
RealToxicityPrompts	10%	1	0.144 (0.01)	0.365 (0.032)	0.254 (0.015)	0.655 (0.022)	0 (0)
		2	0.128 (0.011)	0.534 (0.048)	0.418 (0.012)	0.773 (0.018)	0.695 (0.02)
		3	0.127 (0.013)	0.58 (0.06)	0.458 (0.017)	0.822 (0.016)	0.625 (0.028)
		4	0.123 (0.013)	0.604 (0.064)	0.489 (0.011)	0.855 (0.015)	0.574 (0.026)
		5	0.121 (0.011)	0.616 (0.059)	0.507 (0.01)	0.873 (0.02)	0.543 (0.022)
	20%	1	0.265 (0.022)	0.35 (0.032)	0.264 (0.015)	0.65 (0.025)	0 (0)
		2	0.247 (0.015)	0.522 (0.029)	0.424 (0.016)	0.772 (0.019)	0.671 (0.012)
		3	0.252 (0.02)	0.598 (0.06)	0.473 (0.023)	0.815 (0.019)	0.599 (0.03)
		4	0.251 (0.016)	0.642 (0.054)	0.512 (0.024)	0.853 (0.02)	0.551 (0.019)
		5	0.249 (0.011)	0.669 (0.051)	0.537 (0.026)	0.877 (0.019)	0.524 (0.027)
	50%	1	0.594 (0.022)	0.347 (0.035)	0.292 (0.031)	0.652 (0.02)	0 (0)
		2	0.639 (0.02)	0.472 (0.034)	0.37 (0.03)	0.703 (0.018)	0.579 (0.013)
		3	0.599 (0.012)	0.634 (0.024)	0.53 (0.021)	0.807 (0.013)	0.589 (0.034)
		4	0.587 (0.013)	0.672 (0.023)	0.572 (0.018)	0.854 (0.012)	0.545 (0.032)
		5	0.581 (0.009)	0.7 (0.015)	0.602 (0.018)	0.879 (0.012)	0.512 (0.03)
Stereoset	10%	1	0.101 (0.019)	0.288 (0.064)	0.141 (0.011)	0.418 (0.025)	0 (0)
		2	0.099 (0.009)	0.432 (0.111)	0.218 (0.046)	0.543 (0.022)	0.648 (0.04)
		3	0.101 (0.009)	0.495 (0.1)	0.246 (0.041)	0.619 (0.034)	0.598 (0.039)
		4	0.103 (0.011)	0.532 (0.096)	0.259 (0.037)	0.669 (0.039)	0.566 (0.037)
		5	0.103 (0.011)	0.552 (0.09)	0.268 (0.036)	0.706 (0.038)	0.537 (0.046)
	20%	1	0.213 (0.031)	0.298 (0.058)	0.139 (0.01)	0.398 (0.024)	0 (0)
		2	0.209 (0.017)	0.474 (0.131)	0.226 (0.058)	0.525 (0.021)	0.633 (0.039)
		3	0.208 (0.018)	0.526 (0.119)	0.252 (0.05)	0.603 (0.039)	0.584 (0.044)
		4	0.207 (0.019)	0.55 (0.12)	0.265 (0.046)	0.655 (0.04)	0.554 (0.038)
		5	0.205 (0.018)	0.565 (0.111)	0.275 (0.042)	0.7 (0.049)	0.53 (0.038)
	50%	1	0.525 (0.023)	0.292 (0.021)	0.14 (0.011)	0.411 (0.041)	0 (0)
		2	0.546 (0.016)	0.639 (0.141)	0.291 (0.059)	0.518 (0.029)	0.583 (0.043)
		3	0.544 (0.019)	0.662 (0.126)	0.303 (0.052)	0.574 (0.041)	0.535 (0.052)
		4	0.539 (0.015)	0.673 (0.117)	0.311 (0.049)	0.623 (0.052)	0.513 (0.054)
		5	0.537 (0.013)	0.689 (0.104)	0.32 (0.044)	0.66 (0.059)	0.492 (0.061)

Table 6: Additional results for our proposed scan2 top- k method on auditing OPT layer 24 on Hallucinations (hall), Stereoset (stereo) and RealToxicityPrompts (toxic). Results for scan2 for different k . Mean (std) results from 10 random test datasets, with best (significant) results in bold. Results for test sets with different percentages of anomalous data (Anom). We report the subset size of sentences (S) and the subset of nodes (N), as well as the intersection of the returned subset of nodes (INode) between the k -th and $(k - 1)$ -th run.

In terms of performance, for Hallucinations precision tends to decrease as the value of k increases, while recall increases with larger values of k . This rise in recall is expected, given that a higher value of k leads to the union of more scans, resulting in a larger subset size. Consequently, the larger the subset size, the higher the likelihood of capturing all anomalous data, thus leading to an increase in recall. The decrease in precision is also expected. At each increment of k , we systematically remove the previously identified subset, which we anticipate to contain a significant portion of anomalous data. For instance, when examining Hallucinations with a test dataset containing 10% of anomalous data, for $k = 1$, we observe a mean precision of 0.813. This suggests that more than 80% of the retrieved instances are true positives. Consequently, for $k = 2$, there is a substantial drop in precision as this initially identified subset is removed from the test set. At this point, the test set no longer contains 10% of anomalous data but considerably less, given that we have removed a subset roughly equivalent to 5% (Size (S))¹⁰ of the training data and consisted of more than 80% anomalous data (Precision). Furthermore, the remaining anomalous data in the dataset might not demonstrate as clear patterns as the removed subset, potentially contributing to a decline in precision. Interestingly, for RealToxicityPrompts and Stereoset we do not necessarily observe such a strong trend, where sometimes, we see an increase in precision for an increase from $k = 1$ to $k = 2$ or $k = 3$ and a consequent drop in precision for larger k .

Regarding the size of the subset of nodes returned (Size (N)), we observe that even at a value of k that strikes a balance between precision and recall, a substantial subset of nodes responsible for flagging the union subset as anomalous is still returned. This finding suggests that there may be a sizable subset of nodes responsible for encoding the investigated bias. For instance, in the case of Hallucinations with a test set containing 20% anomalous data, top-3 results yield a mean precision of 0.412 and a mean recall of 0.736, while returning an average of 0.613 nodes as a subset.

However, this phenomenon can also be explained by the sequential subset removal process. At each step k , we might identify a distinct anomalous pattern, potentially encoded in different nodes. Looking at the intersection of nodes between k and $k - 1$ for $k \in 2, 3, 4, 5$, we notice a tendency where approximately 50% of the nodes from step $k - 1$ tend to be included in step k . However, when considering the increase of node subset size (Size (N)) between $k - 1$ and k , it appears that each k adds a larger number of additional nodes. For example, consider the case of Hallucinations with a test set containing 20% anomalous data. At the top-2 level, we find roughly 30% of the nodes, while at the top-3 level, we identify just above 60% of the nodes.

E.6 Outlook: Analyzing the Returned Subset of Nodes

In this section, we show corresponding preliminary results for the potential expansion of our work as discussed in § 5. As introduced in § 2, our method returns the subset $S^* = Z_S \times O_S$, where Z_S refers to the subset of test samples (sentences) and O_S to the subset of nodes for the layer analyzed. In the main paper, we assess whether the subset of sentences Z_S , which yield LLM embeddings identified as anomalous, align with the bias under examination and report precision and recall and relative sample subset size. In this context, our focus was on bias detection, specifically during the auditing process.

We seek to expand our research by exploring bias mitigation strategies. We believe that an examination of the subset of nodes O_S could provide valuable insights. O_S represents the collection of nodes that correspond to the most anomalous subset of sentences—those nodes whose empirical p -values of activations deviate from the uniform distribution, thereby flagging them as anomalous. We hypothesize these nodes are pivotal in identifying anomalous patterns within the data, which could guide the efficient fine-tuning of sub-networks for bias mitigation.

Exploring the Subset of Nodes In Figure 2, we present the node frequency in the subset obtained under varying compositions of test data for the Hallucinations dataset. The plot illustrates how frequently nodes appear in the resulting subset across 10 randomly generated test datasets, each containing different percentages of anomalous (false) statements, specifically 10%, 20%, 50%, 80%, and 90%. Results are for auditing the OPT 6.7b model, activations from layer 20, and scanning under the Higher Criticism scoring function for left-tail, right-tail, and top-1 2-tailed p -values.

We observe that the lower the amount of anomalous data in the test set, the number of nodes that are returned at high frequency. Specifically, when the test data contains only 10% anomalous data,

¹⁰Note, this is the aggregated subset size over top- k runs, and not the size returned by the individual runs.

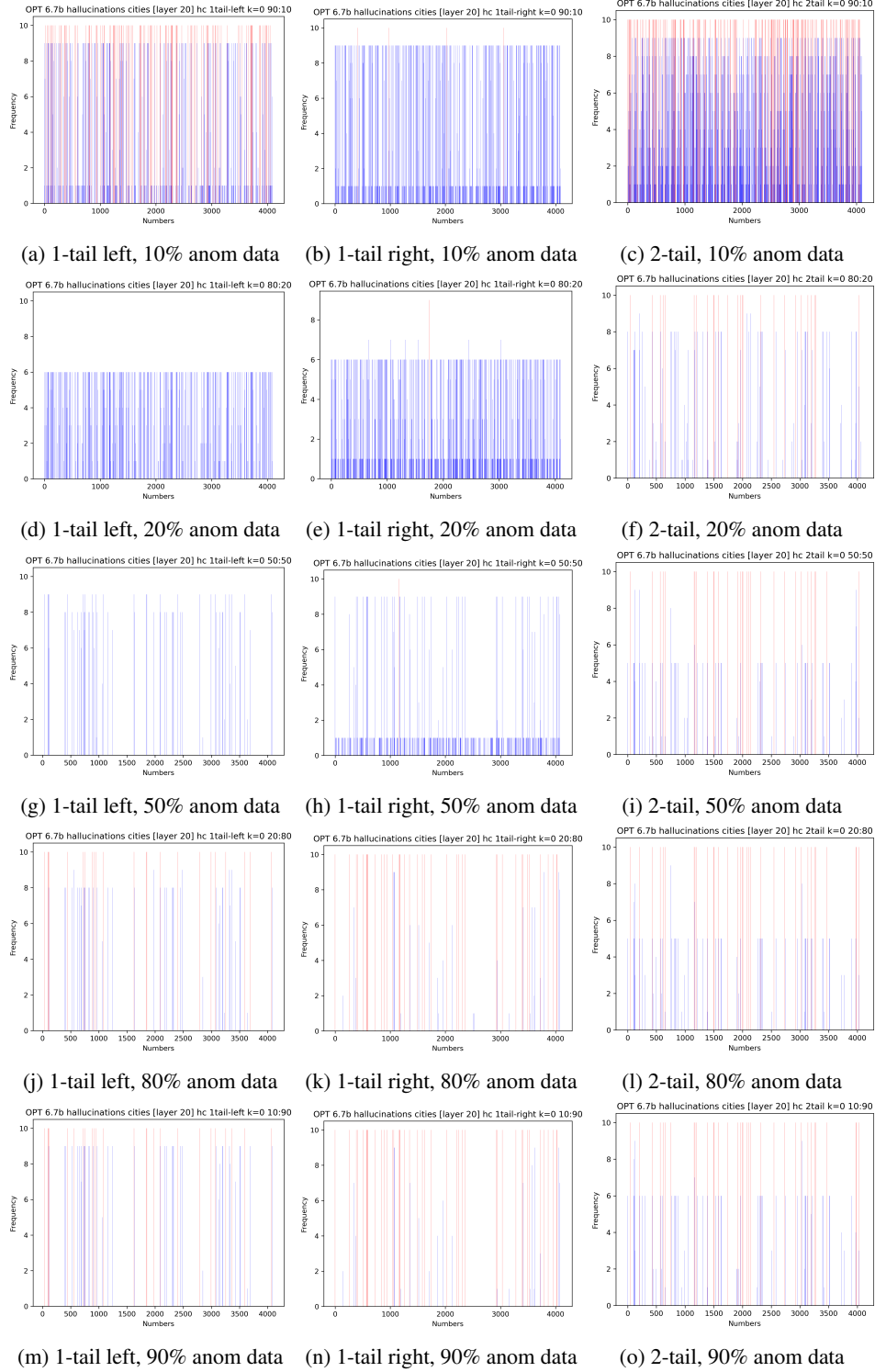


Figure 2: Frequency of nodes in the returned subset of nodes for test datasets containing different amounts of anomalous data across 10 random test sets for Hallucinations data. Red: nodes that are returned for all 10 test sets. Results for OPT 6.7b model, activations from layer 20, using the Higher Criticism scoring function.

we consistently find a high number of nodes being returned at least in 9 out of 10 random test sets scanned (Fig. 2a - 2c). However, as the percentage of anomalous data in the test set increases to 50% or higher (Fig. 2g - 2o), we observe a clear reduction in the number of nodes returning at such frequencies. Further, in most cases, nodes tend to either appear 9 or 10 times or not at all. This pattern could be attributed to the scanning method’s growing confidence in identifying the anomalous pattern as the subset size increases, leading to a more focused identification of critical nodes.

This observation suggests that when the scanning method gains confidence in pattern detection, it becomes more selective in attributing anomalous activations to a smaller number of nodes. Fine-tuning efforts could be efficiently directed toward training these identified critical nodes. Note that while this trend holds for various p -value calculations, the specific frequencies and numbers of returned nodes vary among the different p -value calculations (columns of Fig. 2).

We now compare results across datasets. In Figure 3 we plot the frequency of each node returned as anomalous for layer 20 of OPT 6.7 2-tailed p -values on the Hallucinations, Stereoset, and RealToxicityPrompts dataset with a test dataset of 80% anomalous data. We highlight those nodes that are found in O_S across all 10 random test sets in red.

In the case of RealToxicityPrompts (toxic) and Stereoset (stereo), we observe a consistent trend across datasets: as the quantity of anomalous data increases, more nodes are either included in the anomalous subset across all test sets or are not included at all/included at very low frequencies.

Consistent with our previous observations, this implies that as the scanning method becomes more confident in pattern detection, particularly evident with larger amounts of anomalous data in the test dataset, it tends to exhibit greater selectivity in ascribing anomalous activations. However, notably, in the cases of RealToxicityPrompts and Stereoset, this selectivity extends to a larger number of nodes than for Hallucinations.

Informing Fine-Tuning Partial fine-tuning has been proposed as an efficient method that preserves model generalization while customizing pre-trained language models (LLMs) for specific tasks [51, 54]. We believe that identifying pivotal nodes responsible for encoding bias may inform partial fine-tuning processes for bias mitigating in LLMs. Note that the definition of bias mitigation depends on the context and stakeholders involved.

For example, to ensure that an LLM remains impartial to stereotypes, we might seek to fine-tune the LLM so that it is indifferent to gender stereotypes, randomly generating both, stereotypical output (e.g., “She spent too much time on makeup.” [40]), and anti-stereotypical output (e.g., “She was fixing her car.” [40]). This process may involve having these pivotal nodes “unlearn” stereotypical patterns.

Conversely, in other (perhaps most) cases, we may aim to empower an LLM to detect instances where it is generating toxic content, hallucinations, or reproducing stereotypes. In this situation, our focus in the fine-tuning process may be on improving the encoding (or “learning”) of harmful patterns within these crucial nodes, such that we can subsequently deploy effective bias mitigation strategies. This approach would align with the concept that the better we become at identifying bias before releasing generated content or predictions, the more effectively we can provide safer and more responsible model behavior.

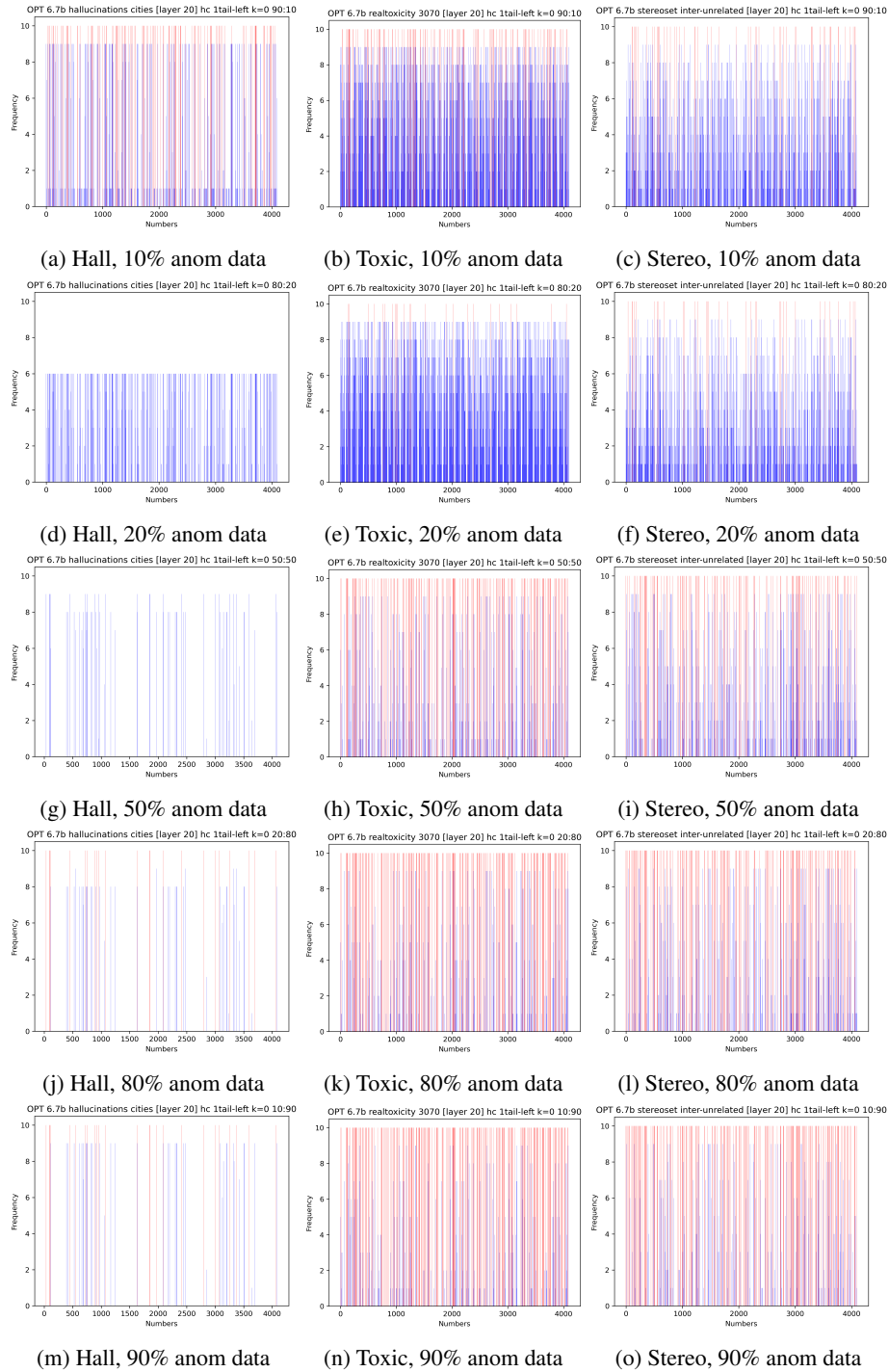


Figure 3: Frequency of nodes in the returned subset of nodes for test datasets containing different amounts of anomalous data across 10 random test sets for Hallucinations (Hall), RealToxicityPrompts (Toxic), and Stereoseg (Stereo) data. Results for OPT 6.7b model, activations from layer 20, using Higher Criticism scoring function, and left-tailed p -values.